Scientific paper

Calculation of the Absorption Spectrum from an ATR Infrared Experiment

Barbara Grobelnik and Jože Grdadolnik*

National Institute of Chemistry, Hajdrihova 19, Ljubljana, Slovenia

** Corresponding author: E-mail: joze.grdadolnik@ki.si*

Received: 05-05-2008

Dedicated to the memory of Professor Ljubo Golič

Abstract

The most efficient and precise method for separation of absorption and reflection contributions in the ATR (attenuated total reflection) spectrum is the calculation of pure absorption spectrum from optical constants. However, the precision of calculated optical constants depends on the alignment of the optical component of an ATR attachment. The arrangement of the ATR attachment always produces imperfections in optical path alignment. Therefore, we calculated the expected error analytically. The calculated error of R_s and R_p is in the range between 3%–8% per deviation of the incidence angle of 1°. To reduce the error of calculated reflectivities, a new procedure for recording the ATR spectrum is proposed. It is based on the calibration of the number of reflection by probing the spectrum of pure liquid water. The proposed procedure significantly reduces the error (< 2%) due to a divergence of the incidence angle. This approach is included in the program for routine calculation of the optical constants and absorption spectra of anisotropic solutions. A structural analysis of three dipeptides in water solutions is shown as an example of the application of an ATR attachment and the calculation of the absorption spectrum. The calculated spectra of dipeptides and bulk water provide ideal conditions for reliable subtraction. The OH stretching region in the difference spectrum of the leucine dipeptide shows characteristic patterns of rearranged water molecules in the vicinity of solutes. From the positions of negative and positive bands we hypothesize that the presence of leucine molecules creates a denser structure of water molecules near the solutes. The modelling of the amide III band shape in the spectra of the methionine and asparagine dipeptide in water reveals the conformation of the dipeptide backbone. The methionine dipeptide possesses mainly the PP_{II} conformation, while the asparagine dipeptide is mostly in the β conformation. The population of α_R is small in both dipeptides.

Keywords: Infrared spectroscopy, ATR experiment, calculation of optical constants, anisotropic solutions, preferential dipeptide conformations

1. Introduction

The use of infrared spectroscopy for the study of chemical and biophysical systems has accelerated in the past few years. Besides its very simple application and universality, the frequencies of bands and the band shapes are directly related to microscopic physical quantities. The growth in these areas, and especially in the field of solution chemistry and biochemistry, has been mainly due to the application of ATR (attenuated total reflection) techniques. With the proper use of ATR attachments, solutions can be studied in very low concentrations without solvent saturation. The biologically relevant systems can be studied in physiological environments with excellent reproducibility and sensitivity. The origin of ATR spectroscopy is rooted in the existence of an evanescent wave of infrared radiation in a lower index of refraction medium in contact with an optically denser medium in which a propagating wave undergoes total internal reflection. The infrared beam is partially absorbed in the medium with a lower index of refraction yielding a typical ATR spectrum. However, an ATR spectrum possesses reflection features in addition to the absorption features[1–3]. Moreover, wavelength dependence is observed for thick samples where spectra are recorded at angles greater than the critical one. In order to avoid the described spectral distortions in recorded ATR spectra, the pure absorption spectrum should be calculated. Therefore, we need an accurate method for calculation of the pure absorption spectrum.

In this paper we will describe a program for calculating the optical constants written in the Matlab environment. In addition to the program description, an analysis of the expected error of calculation will be presented. Water solutions of leucine, methionine and asparagine dipeptide will be used as examples of the calculation of an absorption spectrum using these techniques.

2. Materials and Methods

Asparagine, leucine and methionine amino acids, blocked by CH_3–CO– and –NH–CH_3 groups (N-acetyl-amino acid-N'-methyl amides; dipeptides), were purchased from Bachem. The samples were prepared in mQ H_2O in concentrations of 0.1 M (methionine, leucine), and 0.03 M (asparagine). The spectra were measured on Perkin-Elmer System 2000 and Bruker FTS-66 infrared spectrometers. Spectra were recorded in the region between the 7000 cm^{-1} and 370 cm^{-1}. Typically, 256 scans were averaged and apodized with a triangular function. The spectra were recorded at 30 °C using a diamond ATR cell equipped with KRS-5 lenses. The subtraction of the spectrum of bulk water was carried out using Grams© software. The amide III band was analyzed using the Grams© and Razor© band fitting procedures. The shape of individual components is modeled with the convolution of a Lorentzian and Gaussian profile, leading to a so-called Voigt profile. The Voigt profile of band shape in a spectrum of solutions is a result of the time scale of the interactions with which vibration relaxation occurs[4].

3. Results and Discussion

3. 1. Calculation of Optical Constants

The utilization of the ATR set up with one internal reflection (Golden Gate) or with three internal reflections (CIRCLE cell) allows the examination of the complete mid infrared region without the saturation of the water OH stretching band. However, an anomalous dispersion significantly alters the spectrum recorded in ATR mode. The frequency differences between the calculated and original ATR bands are large, especially for strong bands (ν OH of water shifts for 56 cm^{-1} and Amide I band shifts for 9 cm^{-1}, see ref.[5]). Moreover, the band shape is also modified. Therefore, it is necessary to calculate a pure absorption spectrum. The optical constants of materials can be precisely determined by combining measurements made at different angles of incidence. Most commercially available ATR accessories have a fixed position for the incident angle. However, instead of two independent measurements at two different angles, an alternative procedure called the Kramers-Kronig (K–K) method was used. Optical constants and the related absorption or ε'' spectra were calculated using a method proposed by Bertie and Lan[6] and Bertie and Eysel[7] in a Matlab© environment. The missing part of the spectra in the far-infrared region was substituted by a descent Gaussian function. The method is based on the interdependence of the optical constants by an integral relationship and on the use of Fresnel's equations. In general, the K–K transformation connects the frequency dependent imaginary and real physical quantities using integral equations.

For a detailed analysis and a comparison between the calculated reflectivity (R) and experimental ATR spectrum we have to know their interdependence. The most easily solved equations are known for the geometry of CIRCLE and Golden gate ATR cells, where θ, the angle of incidence, is 45° and where reflectivity in both polarizations are related as $R_s^2 = R_p$ (Ref.[8]). This relationship is used during an iterative procedure of calculating the n and k by K–K transformation and by comparing the calculated values with the original ATR spectrum. In general, the system of Fresnel equations must be solved for the given optical system in order to obtain the relationship between the spectrum and reflectivity. Equations 1 to 10 describe the typical approach used to calculate the optical constants from the experimental spectrum.

$$R_s = \frac{n_1^2 \cos^2\theta - 2an_1\cos\theta + Y}{n_1^2 \cos^2\theta + 2an_1\cos\theta + Y}, \quad (1)$$

where

$$Y = \left(\left(n_2^2 - k_2^2 - n_1^2\sin^2\theta\right)^2 + 4n_2^2k_2^2\right)^{1/2} \quad (2)$$

$$a = \frac{1}{\sqrt{2}}\sqrt{X+Y} \quad (3)$$

and

$$X = n_2^2 - k_2^2 - n_1^2\sin^2\theta. \quad (4)$$

R_p is expressed as

$$R_p = R_s\frac{n_1^2\left(\sin^2\theta\right)tg^2\theta + Y - 2an_1\left(\sin\theta\right)tg\theta}{n_1^2\left(\sin^2\theta\right)tg^2\theta + Y + 2an_1\left(\sin\theta\right)tg\theta}. \quad (5)$$

The experimental ATR spectrum, where $\theta = 45°$ is expressed as a function of R_s ($R_p = R_s^2$) as:

$$ATR = -\log_{10}\left[\frac{\left(R_s^m + R_s^{2m}\right)}{2}\right]. \quad (6)$$

n_1 and k_1 are the optical constant of bearing crystal, and n_2 and k_2 the optical constants of sample. A complex dielectric constant ($\hat{\varepsilon}_2 = \varepsilon_2' + i\varepsilon_2''$) is connected with a complex optical constant ($\hat{n}_2 = n_2 + ik_2$) as:

$$\hat{n}_2^2 = \hat{\varepsilon}_2, \quad (7)$$

$$\varepsilon'' = 2n_2k_2, \quad (8)$$

and

$$\varepsilon'_2 = n_2^2 - k_2^2. \quad (9)$$

Equation (6) is valid for both the Golden gate and CIRCLE ATR attachment. The absorption spectrum is finally calculated as

$$A = 2\pi k_2 \tilde{\nu} d \quad (10)$$

where d is sample thickness and $\tilde{\nu}$ is wavenumber (cm^{-1}). The program used for the calculation of optical constants and absorption spectrum is available on request.

3. 2. Calculation of the Main Contribution to the Error of Determined Optical Constants

The main source of error in applying the described procedure is the deviation in the incidence angle of the infrared light. This type of error cannot be avoided even with accurate tuning of the optical path of the infrared beam. Therefore, the calculation of the resulting error is important in estimating the overall accuracy of the presented calculation. The expression for reflectivity is expanded around the θ angle. Thus we get two equations for R_s and R_p reflectivities.

$$\frac{\partial R_s}{\partial \cos(\theta)} = \frac{2}{\frac{1}{2}n_1^2 + Y + \sqrt{2}an_1}\left(an_1^3 - 2Yn_1 + \frac{2a}{Y}n_1^3\left(n_2^2 - k_2^2 - \frac{n_1^2}{2}\right) - \frac{n_1^3}{2a}\left(Y + \frac{n_1^2}{2}\right)\left(1 + \frac{n_2^2 - k_2^2 - \frac{n_1^2}{2}}{Y}\right)\right) \quad (11)$$

From the known relationship between R_p and R_s we can calculate a similar expression for

$$\frac{\partial R_p}{\partial \cos(\theta)}:$$

$$\frac{\partial R_p}{\partial \cos(\theta)} = \frac{2R_s}{\left(\frac{1}{2}n_1^2 + Y + \sqrt{2}an_1\right)^2}\left(-2an_1^3 + 4Yn_1 + \frac{4a}{Y}n_1^3\left(n_2^2 - k_2^2 - \frac{n_1^2}{2}\right) - \frac{n_1^3}{2a}\left(Y + \frac{n_1^2}{2}\right)\left(1 + \frac{n_2^2 - k_2^2 - \frac{n_1^2}{2}}{Y}\right)\right) \quad (12)$$

It is inconvenient to estimate the magnitude of error from the long analytical expressions presented in equations (11) and (12). The expansion of Fresnel equation for absorbing media round $\theta = 45°$ yields for both polarizations the following expression:

$$R''_{s,p} = R_{s,p}(45°) + \left[\frac{\partial R_{s,p}}{\partial \cos(\theta)}\frac{\partial \cos\theta}{\partial \theta}\right]_{\theta=45°}\Delta\theta, \quad (13)$$

which can be rearranged as

$$\frac{R''_{s,p}}{R_{s,p}(45°)} - 1 = \frac{1}{R_{s,p}(45°)}\frac{\partial R_{s,p}}{\partial \cos(\theta)}\frac{\partial \cos\theta}{\partial \theta}\Delta\theta. \quad (14)$$

The maximal error in the calculation of R_s and R_p is relatively small. A variation of incident angle by 1° produces the maximal relative error in R_s at slightly above 3%. It is even smaller for k_2 values round 0.3 (Fig. 2), which are characteristic for water solutions. However, the relative error is small only if deviations in the angle of incidence beam are small. In practices, the value of $\Delta\theta$ is, rather than 1°, closer to several degrees, which already significantly alters the values of the calculated optical constants. Therefore, a reduction in the described error is necessary for accurate determination of the absorption spectrum.

3. 3. Optimization of the Number of Reflections m

Equation (6) is valid only for an incidence angle θ = 45°, where $R_s^2 = R_p$ (Ref.[8]). The parameter m gives the number of internal reflections. Theoretically, in the case of the ATR diamond attachment (Golden gate), m should be equal to 1 and 3 in the case of CIRCLE ATR attachment. However, in practice, the value of m is always less than expected by theory. The reason lies in imperfect alignment of the ATR accessories. The incidence beam is not completely parallel and thus the incidence angle deviates from the ideal value. However, this divergence in the incidence angle can be used for fine-tuning of the calculations for the optical constants.

To achieve a better description of the optical path of the infrared beam in the ATR experiment, the spectrum of mQ H_2O was recorded prior every recording. The optical constants for bulk water are precisely known[9] and therefore can be used as a calibration standard for calculating the actual number of internal reflections. We use Equation (8) and optimize the calculated ATR spectrum from the known optical constants of water by applying equation (1) and the relationship between the dielectric functions and optical constants. The only fitting parameter is m, the number of internal reflections. In an aligned ATR dia-

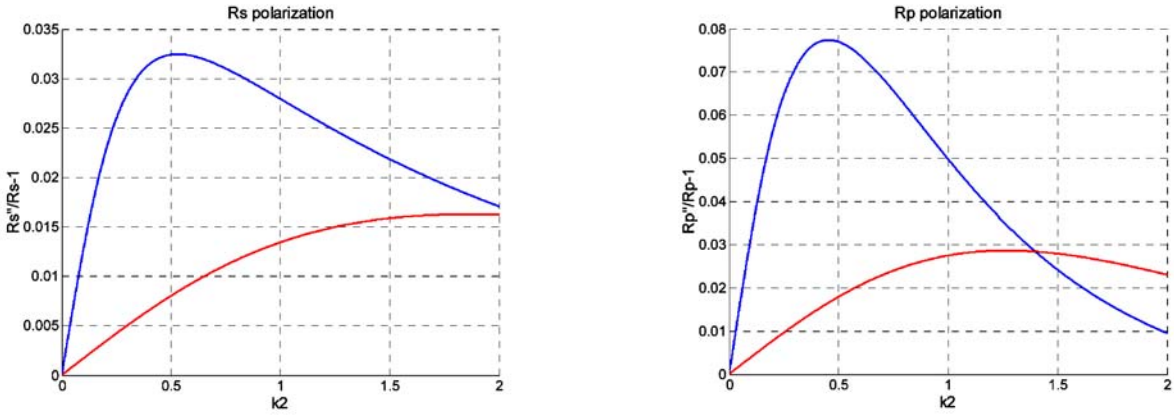

Figure 1. The R_s"/R_s-1 and R_p"/R_p-1 as a function of k_2 for germanium (n_1 = 4.0, upper line) and diamond (n_1=2.4, lower line) bearing crystals. The n_2 is equal 1.33 (liquid water). The incident angle (θ) is 45° and $\Delta\theta$ is ±1°.

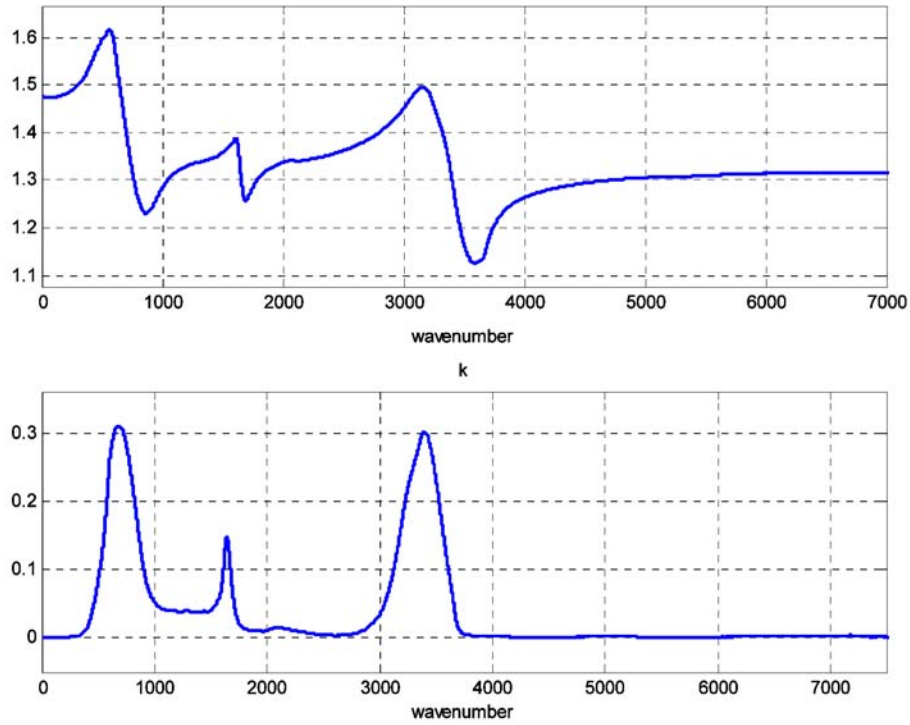

Figure 2. Calculated n_2 and k_2 for asparagine dipeptide in H_2O.

mond attachment *m* appears to be between 0.89 and 0.97. The optimized number of internal reflections for the CIRCLE ATR attachment lies in a range between 2.78 to 2.92. By applying the corrected number of internal reflections, the absolute errors of n and k are significantly reduced. They stay in the range up to 2%.

3. 4. Spectrum of Leucine Dipeptide in Water

Water is known as extremely good absorber and thus classical transmission techniques often lead to saturation of absorption bands. The saturation makes the OH stretching region of no use in original as well as difference spectra of water solutions and bulk water. The saturation of the most intense bands leads to nonlinearity in the infrared detector and prevents the proper subtraction of solvent. The application of ATR technique eliminates saturation and allows accurate subtraction even in the region of OH stretchings.

Figure 3 shows the spectrum of leucine dipeptide in water after the subtraction of bulk water (the subtraction factor is 0.938). The main guides to proper water subtraction were intensity and shape of the baseline in the regions with no significant contributions of absorption bands. In these regions the baseline should be flat and close to zero

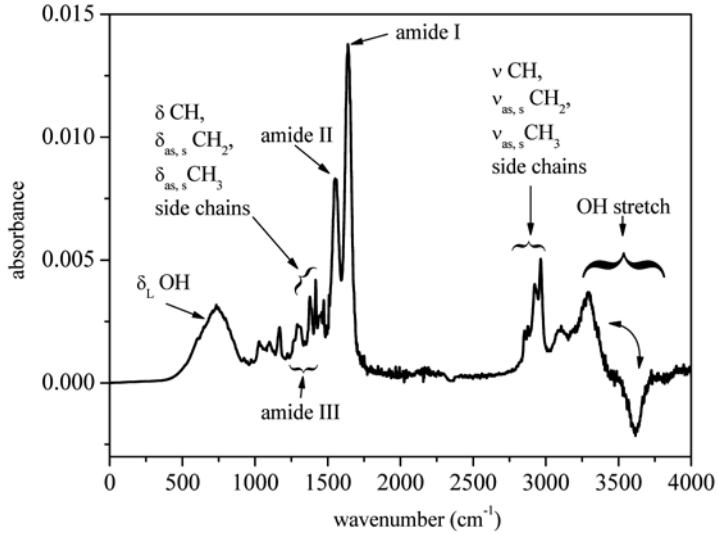

Figure 3. The difference spectrum of leucine in H_2O solution after subtraction of bulk water.

intensity. The original ATR spectra of leucine solution and bulk water were used to calculate the absorbance spectra, which were further applied in the subtraction procedure. Elimination of the bands due to the presence of bulk water in solution simplifies the infrared spectrum. Moreover, the subtraction reveals the typical differential bands in the region of OH stretching (νOH) between 3000 cm^{-1} and 3600 cm^{-1}. This structure of νOH bands with positive and negative intensities is characteristic for showing the changes in the strength of intermolecular interactions between the particular vibrating groups[10–12]. The band at 3620 cm^{-1}, characteristic for very loosely hydrogen-bonded or almost free OH groups, is more intense in the spectrum of bulk water than in the spectrum of dipeptide solution. In contrast, the band at 3290 cm^{-1} is more intense in the spectrum of the dipeptide solution than in the spectrum of bulk water. This band represents the vibration of OH groups, which participate in hydrogen bonds of moderate strength. Note that the maximum νOH of bulk water[5] is at 3406 cm^{-1}. The appearance of both negative and positive bands in the vibrational spectrum can be explained in terms of the changing strength of hydrogen bonds of those OH groups of water, which are near the dipeptide molecules. The solvation of the dipeptide in water reduces the number of weakly hydrogen bonded or almost free OH groups. These OH groups form hydrogen bonds of moderate strength; the OH stretching band red shifts by 330 cm^{-1}. The OH stretching band with positive intensity is even red shifted with respect to the νOH band in bulk water (116 cm^{-1}). Therefore, the reformatted hydrogen bonds, which appear only in the solution of the dipeptide, are stronger than those that are the most populated in bulk water. The interaction with the dipeptide proton donors and acceptors and the formation of the cage-like structures around the hydrophobic part of the dipeptide causes an overall denser packing of water molecules. Such a denser water structure can also be found at protein surfaces.[13, 14]

The subtraction can also reveals the most significant bands of the dipeptide. The side chain stretching and deformation modes can easily be assigned to particular vibrations (see Fig. 3). Moreover, the amide I, amide II and amide III bands, which are the most characteristic bands of peptides and proteins, can be used for detailed structural analysis.[15]

3. 5. Preferential Conformations of Dipeptides

Recent NMR[16] and vibrational[15] studies of dipeptides have shown that dipeptides in water possess conformational preferences for the dihedral angles φ and Ψ (β or *C5*: $\varphi \approx -120°$, $\Psi \approx 120°$, *PPII*: $\varphi \approx -75°$, $\Psi \approx 145°$, α_R: $\varphi \approx -60°$, $\Psi \approx 60°$). These studies have shown that backbone conformational preferences vary striking among dipeptides. The physical background for the preferential conformations of dipeptides can be explained by the electrostatic screening (ES) model.[15, 17–22] In the ES model, it is assumed that the total free energy of an amino acid residue is determined predominantly by the local electrostatic energy of the backbone dipole moments (N–H and C=O) due to interactions with neighboring peptide groups and by the solvation free energy of the backbone dipole moments.[17] According to this model, the β conformer is energetically more favorable than the α_R state of a residue in gas phase. The anti-parallel orientation of the backbone dipole moments stabilizes the β conformer and the parallel orientation of dipole moments destabilizes the α_R conformer. However, the parallel arrangement of dipole moments in the α_R state has advantages in a polar solvent because of favorable interactions with the solvent. Conse-

quently, the solvation of backbone atoms is much larger for the α_R than for the β conformers. Solvent stabilization thus screens the destabilization of the α_R state due to peptide dipole moments. Modulation of the screening of backbone electrostatic interactions by side chains thereby cause different conformational preferences of residues in aqueous solutions.

3. 6. Amide III Region

The Amide III bands (Fig. 4) appear in the spectrum of proteins as moderately intensive band(s) in the region between 1320 cm^{-1} and 1240 cm^{-1}. This vibration arises mainly due to the N–H in-plane bending coupled to some other peptide modes (C–N stretching, C–C stretching, and C–O in-plane bending). Sensitivity of the Amide III band components to the change in conformation has been proven by numerous experimental and theoretical studies.[15, 23–29] These studies show that the frequency of the Amide III band depends on both dihedral angle φ and Ψ.

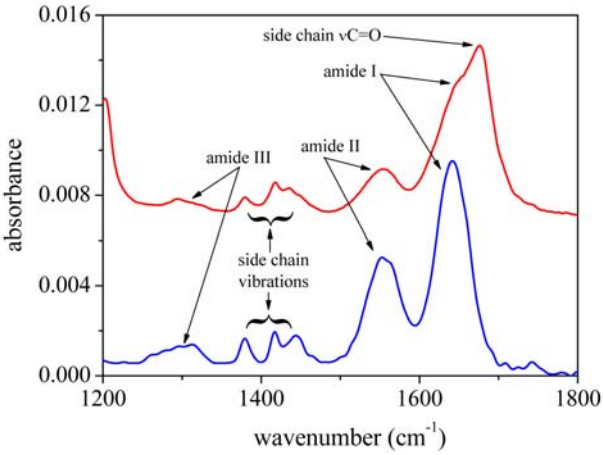

Figure 4. The amide I, II and III spectral regions of asparagine (upper spectrum) and methionine (lower spectrum) dipeptides after subtraction of bulk H_2O.

The spectra of the Amide III regions of methionine and asparagines dipeptides (Fig. 5.) show three components near 1310 cm^{-1}, 1300 cm^{-1}, and 1280 cm^{-1}. A theoretical study by Mirkin and Krimm[30] predicts the characteristic frequency of the Amide III band of the α_R conformation to be near 1290 cm^{-1}; therefore, we assigned the band at 1300 cm^{-1} to the α_R conformation. Analogous to other studies,[15, 23–25, 27, 29–31] we assigned the low frequency component to the β conformation and the high frequency component to the PP_{II} conformation. Assuming equal values of extinction coefficients for all three components, we can calculate the conformational populations from the band areas. Thus, the methionine dipeptide possesses mainly PP_{II} conformation (50%), while β and α_R are less populated (47% β and 3% α_R). The structural analysis of Amide III bands revealed that there was a distinct distribution of populations of conformers in asparagine. The most populated is the β conformer (58%) followed by PP_{II} (40%) and α_R (2%).

4. Conclusions

The application of the ATR set up in this experiment has allowed very accurate measurements of substances with high absorption coefficients. With the appropriate calculation of the absorption spectra as presented in this paper, the spectra can be applied for comprehensive conformational studies. This is even true for systems, which have been known as a "poison" for infrared spectroscopy. Typical examples are water solutions. The high absorption coefficient of liquid water causes saturation effects of the OH stretching bands in spectra measured by the classical transmission technique. The application of the ATR attachment, with the appropriate selection of the bearing crystals, allows the saturation effects to be easily avoided. Thus, the whole mid infrared region is available for structural or analytical studies even in cases where the subtraction of the bulk solvent is required. By applying the pro-

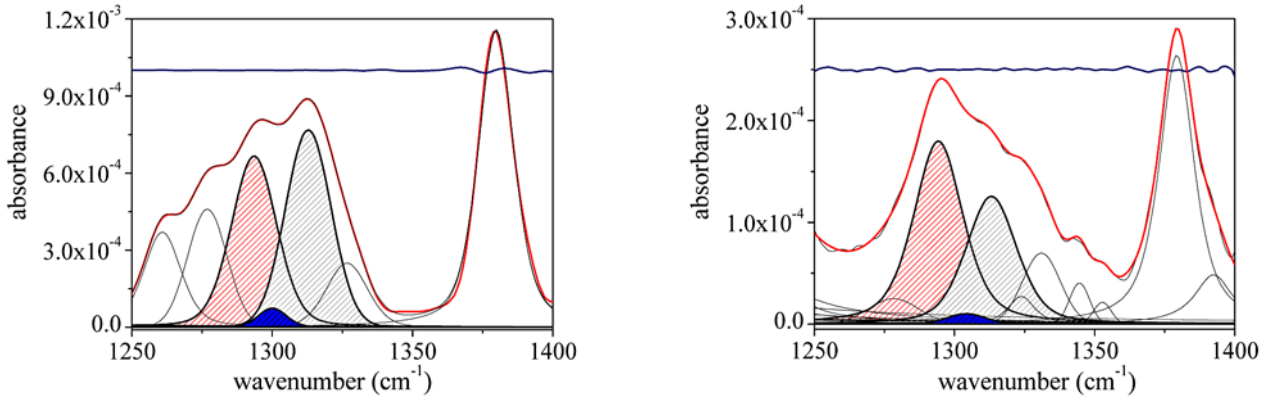

Figure 5. The decomposition of the amide III region of the asparagine dipeptide (right figure) and methionine dipeptide (left figure). Right filled components correspond to β, blacl to α and left filled to PP_{II} conformers. The line at the top of spectra corresponds to the difference between the calculated and measured spectra.

posed program for calculation of the absorption spectrum, these spectra can also be correlated with the ordinary absorption spectra measured in transmission mode. We calculated the expected error of reflectivity due to imperfections in describing the optical path of the infrared beam for both polarizations. The calculated error is between 3 and 8% per change in the incident angle θ by 1°. The proposed application of water as the internal standard and the optimization of the calculation procedure both significantly improve the reliability of the calculated absorption spectrum. The optimization of the number of internal reflections drops the error below 2% even in cases where the deviation of the incident angle is on the order of several degrees.

The excellent quality of recorded and processed spectra allows the detailed application of the vibrational bands for structural and/or analytical studies. The presented examples show the applicability of ATR and calculated spectra for structural studies. The ATR study of dipeptide solutions in water reveals not only the conformation of the dipeptide backbone as a function of the type of side chain, but also the change in the hydrogen bond network of water molecules near the dipeptide molecule.

5. Acknowledgement

We would like to thank Mrs. Silva Zagorc for technical assistance. The authors are indebted to one of the referee for remarks and useful suggestions. This work was supported by the Ministry of Higher Education, Science, and Technology of Slovenia.

6. References

1. Fahrenfort, J. *Spectrochimica Acta* **1961**, *17*, 698–709.
2. Harrick, N. J. *Internal Reflection Spectroscopy*; Interscience Publisher: New York London Sydney, 1967.
3. Mirabella, F. M. *Internal Reflection Spectroscopy. Thoery and Applications*; Marcel Dekker, Inc.: New York, Basel, Hong Kong, 1993; Vol. 15.
4. Meier, R. *Vibrat. spectrosc.* **2005**, *39*, 266–269.
5. Grdadolnik, J. *Acta Chimica Slovenica* **2002**, *49*, 631–642.
6. Bertie, J. E.; Lan, Z. *J. Chem. Phys.* **1996**, *105*, (19), 8502–8514.
7. Bertie, J. E.; Eysel, H. H. *Applied Spectroscopy* **1985**, *39*, (3), 392–401.
8. Born, M.; Wolf, E. *Principles of Optics*; University press: Cambridge, 2005.
9. Bertie, J. E.; Ahmed, M. K.; Eysel, H. H. *J. Phys. Chem.* **1989**, *93*, 2210–2218.
10. Grdadolnik, J. *Vibrat. Spectr.* **2003**, *31*, 289–294.
11. Grdadolnik, J.; Maréchal, Y. *Biopolymers (Biospectroscopy)* **2001**, *62*, (1), 40–53.
12. Grdadolnik, J.; Maréchal, Y. *J. Mol. Struct.* **2002**, *615,* 177–189.
13. Merzel, F.; Smith, J. C. *Proc. Natl. Acad. Sci. U. S. A.* **2002**, *99*, (8), 5378–5383.
14. Merzel, F.; Smith, J. C. *J. Chem. Inf. Mod* **2005**, *45*, (6), 1593– 1599–1599.
15. Grdadolnik, J.; Golič Grdadolnik, S.; Avbelj, F. *J. Phys. Chem. B* **2008**, *112*, 2712–2718.
16. Avbelj, F.; Golič Grdadolnik, S.; Grdadolnik, J.; Baldwin, R. L. *Proc. Natl. Acad. Sci.* **2006**, *103*, (5), 1272–1277.
17. Avbelj, F. *J. Mol. Biol.* **2000**, *300*, 1335–1359.
18. Avbelj, F.; Baldwin, R. L. *Proc. Natl. Acad. Sci. USA* **2002**, *99*, 1309–1313.
19. Avbelj, F.; Baldwin, R. L. *Proc. Natl. Acad. Sci. USA* **2004**, *101*, 10967–10972.
20. Avbelj, F.; Fele, L. *J. Mol. Biol.* **1998**, *279*, 665–684.
21. Avbelj, F.; Luo, P.; Baldwin, R. L. *Proc. Natl. Acad. Sci. USA* **2000**, *97*, 10786–10791.
22. Avbelj, F.; Moult, J. *Proteins: Structure, Function, and Genetics* **1995**, *23*, 129–141.
23. Lord, A., C. *Appl. Spectrosc.* **1977**, *31*, 187–193.
24. Bandekar, J. *Biochim. Biophys. Acta* **1992**, *1120*, 123–143.
25. Fu, N. F.; DeOliviera, D. B.; Trumble, W. R.; Sarkar, H. K.; Singh, B. R. *Appl. Spectrosc.* **1994**, *48*, (11), 1432–1441.
26. Watson, T. M.; Hirst, J. D. *Phys. Chem. Chem. Phys.* **2004**, *6*, 998–1005.
27. Watson, T. W.; Hirst, J. D. *J. Phys. Chem. A* **2002**, *106*, 7858–7867.
28. Schweitzer-Stenner, R.; Eker, F.; Huang, Q.; Griebenow, K.; Mroz, P. A.; Kozlowski, P. M. *J. Phys. Chem B* **2002**, *106*, 4294–4304.
29. Myshakina, N. S.; Asher, S. A. *J. Phys. Chem. B* **2007**, *111*, 4271–4279.
30. Mirkin, N. G.; Krimm, S. *J. Phys. Chem. A* **2002**, *106*, 3391–3394.
31. Burgess, A. W.; Scheraga, H. A. *Biopolymers* **1973**, *12*, 2177–2183.

Povzetek

Najučinkovitejša in zelo točna metoda za ločbo absorbcijskih in refleksijskih prispevkov v ATR (**A**ttenuated **T**otal **R**eflection) spektrih je izračun čistega absorbcijskega spektra iz optičnih constant. Uporaba ATR nam dovoljuje merjenje snovi z visokimi absorbcijskimi koeficienti. Z ustreznim izračunom absorbcijskih spektrov te lahko uporabimo za nadaljnjo konformacijsko analizo tudi v primerih težavnih spektrov. Tipični primeri so vodne raztopine.